

Vis-active TiO_2 – rGO Photocatalysts for Advanced Wastewater Treatment

Ioana TISMANAR¹, Alexandru Cosmin OBREJA², Octavian BUIU², and Anca
DUTA¹

¹Transilvania University of Brasov, Romania

²National Institute for Research and Development in Microtechnologies, Bucharest, Romania

E-mails: ioana.tismanar@unitbv.ro^{*}, a.duta@unitbv.ro,

cosmin.obreja@imt.ro, octavian.buiu@gmail.com

^{*} Corresponding author

Abstract. The implementation of efficient Vis-active photocatalysts, targeting water re-use, represents a priority considering the up-scaling and possible feasible candidates are the composites with metal oxide matrix and graphene derivative(s) fillers. The most efficient metal oxide matrix is titanium dioxide and coupled with the reduced graphene oxide it can develop Vis-active photocatalytic composites. This paper analyzes the performance of these composites as potential photocatalysts to be implemented at industrial scale. The properties of the TiO_2 - rGO composite thin films are discussed along with the efficiencies in degrading the methylene blue standard pollutant; moreover, the stability of these thin films during the photo-degradation processes is outlined correlated with the rGO filler content in the composites.

Key-words: Photocatalyst aqueous stability; TiO_2 – rGO composite thin film; Vis-active photocatalyst.

1. Introduction

The water stress discussed at global scale during the past years outlines the urgent need for developing novel technologies and materials for the advanced wastewater treatment targeting the water re-use and the advanced oxidation processes were intensively investigated, particularly the heterogeneous photocatalysis processes, because of their efficiency in the nonselective degradation of the organic pollutants at low concentration, where the traditional treatment processes are less efficient, [1]. These processes can be implemented in applications aiming at the use of

solar radiation in affordable, low cost processes. The target is to develop photocatalytic materials, using up-scalable methods, that can be activated using solar or visible (Vis) radiation as these types of radiation significantly reduce the overall cost of the process. Good candidates were reported to be the composites with a metal oxide matrix and graphene derivatives fillers as graphene oxide (GO) or reduced graphene oxide (rGO), [2]. Among the ionic semiconductors, titanium dioxide (TiO_2) is the mostly used material in photocatalytic processes, in both laboratory studies and in pilot instalations, mainly because of its high aqueous stability over a broad pH range (pH = 5...9), its low cost and non-toxicity, [3]. However, TiO_2 is a wide band gap semiconductor ($E_g, \text{anatase} = 3.2 \text{ eV}$), thus it can only be activated by UV radiation and it has a high electron-hole recombination rate, [4]. Overcoming these issues additionally leads to the Vis- or solar activation of the photocatalytic material and the strategies involve doping the metal oxide or coupling the UV-active semiconductor with other (narrower) band gap semiconductors with suitably aligned energy bands. These diode (n-p) or tandem (n-n or p-p) structures have also the important advantage represented by the limitation of the electron-hole recombination due to the different migration paths of the charge carrier species.

The trend of coupling an n-type metal oxide with the p-type (r)GO is justified by the unique properties of these carbon-based materials. By coupling with metal oxides (eg. TiO_2), the composites have high efficiencies in the photocatalytic processes due to the limitation of $e^- - h^+$ recombination and can be activated with radiation corresponding to the Vis spectral range, because of the suitable alignment of the semiconductors energy bands, forming n-p (diode type) heterojunctions, [5, 6]. In addition, these composite structures have a high stability in the aqueous environment even at extreme pH values and can be obtained by simple techniques with acceptable cost. Therefore, the composites with graphene derivatives fillers (GO or rGO) are good candidates for meeting the set of requirements for photocatalytic materials. However, there are still challenges to overcome in developing continuous and stable interfaces between the ionic TiO_2 and the slightly polar (r)GO. The filler's polarity has to be considered, especially when using rGO that is less polar than GO due to a lower amount of functional oxide groups. The use of rGO is however recommended as it proves good conduction properties and can work as an electron scavenger, [7].

This paper reports on double-layered composite thin films with TiO_2 matrix and rGO filler. The composites were developed by spray pyrolysis deposition (SPD) to get the first (crystalline) TiO_2 layer followed by spraying the composite TiO_2 - rGO sol as second layer. The composite layers were characterized in terms of crystallinity, morphology, surface composition and roughness and were tested in the photocatalytic degradation of the standard methylene blue, MB, dye, [8], allowing to outline the influence of the rGO content on the composite properties. The stability of the thin films in the working environment was estimated by comparing the characterization results before and after the photocatalytic experiments.

2. Materials and Methods

The composite thin films were deposited as double-layered thin films using glass plates as substrate (1.5cm x 1.5cm) covered with a thin film of fluorine doped tin oxide (FTO glass). The first layer consisted of a TiO_2 thin film deposited using Spray Pyrolysis Deposition (SPD) at 400°C with 30 spraying sequences and 60s break between two consecutive deposition pulses using as precursor system an ethanolic (C_3H_5OH , EtOH) solution of titanium tetra-isopropoxide, ($Ti[OCH(CH_3)_3]_3$, TTIP) and acetylacetone, ($C_5H_8O_2$, AcAc) in a 15:1:1_(V) ratio. After de-

position, this layer was annealed at 450°C for 3 hours to increase its crystallinity degree. This layer has the role to properly support the ordered deposition of the second composite layer of TiO₂-rGO obtained using TTIP, EtOH, AcAc, acetic acid, (CH₃COOH, HAc), water and a rGO ethanolic dispersion. The overall volumic ratio of the reactives in the sol-gel synthesis was TTIP : EtOH : AcAc : HAc : H₂O = 1 : 0.8 : 0.04 : 0.009 : 0.12_(V). The ethanol in the precursor system was replaced with up to 26.3 mg/mL rGO ethanolic dispersion to obtain 0.15%_w, 0.9%_w, 3%_w, 5%_w, 7.5%_w rGO in the composite second layer. The TiO₂ - rGO sols were diluted with ethanol in a sol:EtOH = 1:5(V) ratio and the diluted sols were deposited on the top of the TiO₂ SPD layer at 100°C CC using 15 spraying sequences with 60s break between two deposition pulses to get the glass/FTO/TiO₂/TiO₂-rGO composite thin films. Then the composite structures were thermally treated for 1h at 150°C to remove the volatile possible by-products traped in the thin film without degrading the rGO filler, [9], known to be stable up to 180°C, [10]. Additional experiments were done using the sample with 0.15%_w rGO in the composite layer, finally treated at 200°C to check the thermal stability of the composite at temperatures slightly higher than the stability temperature of rGO.

The composites were investigated in terms of crystallinity (X-ray difraction, XRD, Bruker D8 Discover diffractometer), morphology (scanning electron microscopy, SEM, Hitachi model S-3400 N type II), average roughness (RMS) using atomic force microscopy (AFM, NT-MDT model BL222RNTE) and surface elemental composition using energy dispersive X-ray spectrometry (EDX, Thermo). Further on, the composite thin films were tested in photocatalytic processes using a 10 ppm methylene blue (MB, (C₁₆H₁₈ClN₃S · 2 xH₂O) aqueous solution under UV+VIS radiation mimicking the solar radiation at much lower irradiance value with G_{Total} = 55 W/m² (G_{UV} = 3W/m² and G_{VIS} = 52W/m²). In a typical experiment, the thin photocatalyst film was immersed in 20 mL of the MB solution with a 10 ppm concentration, [8], and left for one hour in dark to reach the adsorption/desorption equilibrium. Then the system was irradiated for 8 hours and the MB removal efficiency was calculated based on the initial solution absorbance and the absorbance after up to 8 hours of irradiation, measured at λ_{MB} = 665 nm, using an UV-VIS-NIR spectrophotometer (Perkin Elmer Lambda 950). Comparative experiments were run using only UV radiation and in dark (without any radiation) to outline the Vis-activation of the composite and the contribution of the adsorption to the MB removal efficiency. The stability of the double-layered composite thin films was evaluated based on the SEM images, the surface elemental composition and the roughness values recorded before and after the photocatalysis experiments.

3. Results and Discussions

The crystallinity results recorded on the sample with the lowest rGO content treated at 150°C and 200°C are presented in Figure 1. The XRD pattern of the first layer (graph (a) in Figure 1) outlines the peaks of TiO₂ (anatase) and the peaks corresponding to the FTO substrate (SnO₂ - cassiterite). The increase in the crystallinity degree in the composite films compared with the TiO₂ film support the idea of an ordered growth of the second layer over the first one although a high temperature treatment was not applied to the double-layered thin films. The characteristic broad peak of rGO is expected at $2\theta = 25.2^\circ$, [11], but the superposition with the TiO₂ peak doesn't allow the filler to be observed. However, the peak at $2\theta = 5.5^\circ$ in Figure 1 (b), (c) can be related to the filler inserted in the TiO₂ matrix. The intensity of this peak lowers with the increase in the temperature applied on the composite thin film. This may be the result of the

partial decomposition/removal of the filler in/from the composite layer.

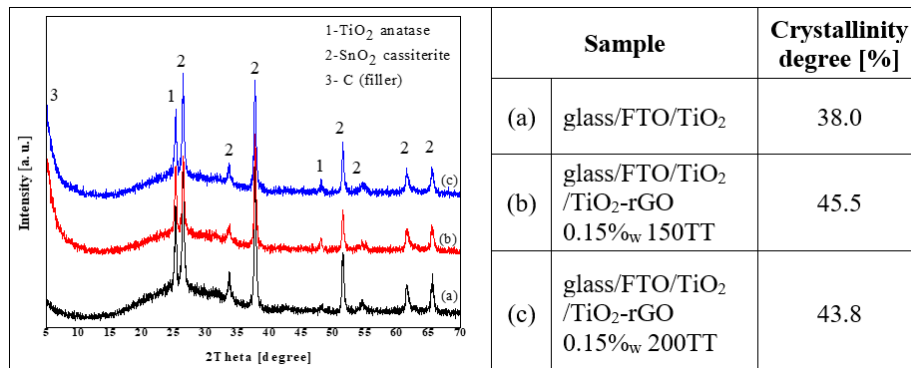


Fig. 1. XRD pattern of the first layer (a) glass/FTO/ TiO_2 and of the composite thin films treated at 150°C (b) glass/FTO/ TiO_2 / TiO_2 -rGO 0.15%_w 150TT and at 200°C (c) glass/FTO/ TiO_2 / TiO_2 -rGO 0.15%_w 200TT.

The morphology of the composite thin films (Figure 2) outlines the rGO platelets covered with TiO_2 aggregates. Fine cracks can be observed around the rGO platelets that are covered with TiO_2 aggregates, thus demonstrating a limited compatibility of the filler with the TiO_2 matrix following the low polarity of the rGO filler.

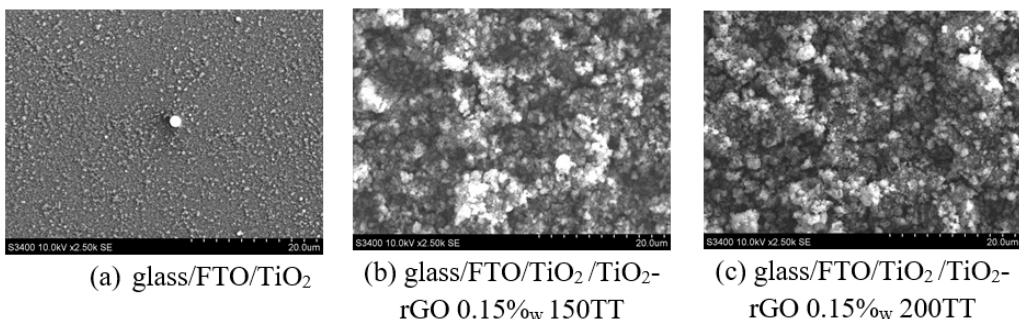


Fig. 2. SEM images of the first layer (a) and of the double-layered composites with 0.15%_w rGO thermally treated at 150°C (b) and at 200°C (c).

However, the carbon content in these composite layers (Table 1) has to be noted. This percentage is lower than expected due to the small percentage of the filler in the thin film treated at 150°C. On the other hand, for the composite treated at 200°C, no carbon content is recorded, concluding that this temperature and higher temperatures than the stability temperature of rGO (180°C) are not recommended as the thermally unstable filler will be decomposed and removed as volatile products from the thin film.

Table 1. Elemental surface composition of the first layer (a) and of the composite layers with 0.15%_w rGO thermally treated at 150°C (b) and at 200°C (c)

Sample	Element [at%]			
	C	Ti	O	F, Sn, Si
(a) glass/FTO/TiO ₂	0.00	24.43	66.66	8.92
(b) glass/FTO/TiO ₂ /TiO ₂ -rGO 0.15% _w 150TT	1.01	34.01	64.54	0.44
(c) glass/FTO/TiO ₂ /TiO ₂ -rGO 0.15% _w 200TT	0.00	35.73	63.60	0.67

Based on these results the content of the filler was raised up to 7.5%_w rGO in the composite layer and the composite thin films were thermally treated at 150°C. The XRD patterns of these thin films are included in Figure 3. The broad characteristic peak of rGO, expected at $2 = 25.2^\circ$, is overlapping with the TiO₂ peaks thus cannot be clearly observed.

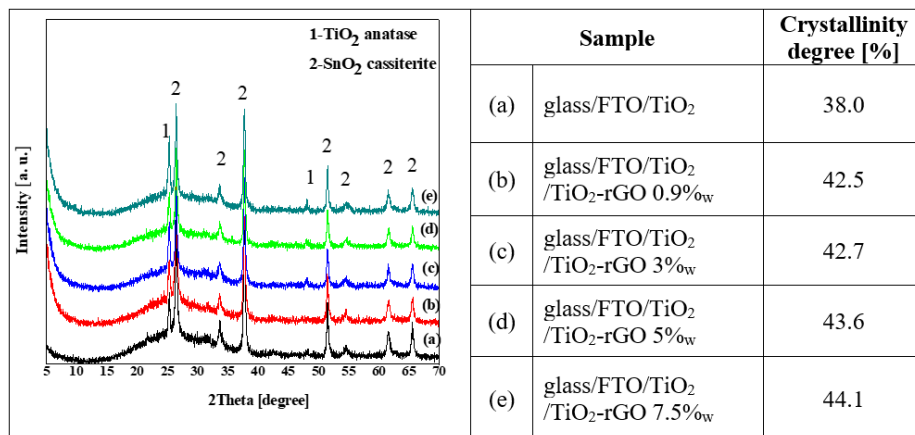


Fig. 3. XRD patterns of the first layer (a) glass/FTO/TiO₂ and of the composite thin films (b) glass/FTO/TiO₂ /TiO₂-rGO 0.9%_w, (c) glass/FTO/TiO₂ /TiO₂-rGO 3%_w, (d) glass/FTO/TiO₂ /TiO₂-rGO 5%_w, (e) glass/FTO/TiO₂ /TiO₂-rGO 7.5%_w.

The crystallinity degree of the composite thin films compared to the TiO₂ thin film supports the idea of an ordered growth of the second layer over the first one, even if no annealing treatment was applied to the double-layered films. The additional peak at $2 = 5.5^\circ$ in Figure 3 (b), (c), (d), (e) may be related to the presence of the rGO filler in the TiO₂ matrix. The XRD patterns of the thin films with higher rGO content are similar with the ones for the sample with very low rGO content (Figure 1). The overall crystallinity degree slightly varies between 42.5...45.5% regardless the filler concentration.

The SEM images in Figure 4 outline the formation of larger aggregates with the increase in the rGO content. The rGO platelets are well covered with TiO₂ aggregates and a more obvious effect can be observed on the 5%_w rGO composite proving that high-performance interfaces between the aggregates and the rGO sheets are developed. However, fine cracks can be observed near the edges of the carbon derivative platelets. The composite with 7.5%_w rGO content has a slightly different morphology with large groups of aggregates stacked at the surface. This can be attributed to the higher filler content that is randomly distributed/aggregated in different areas of the thin film.

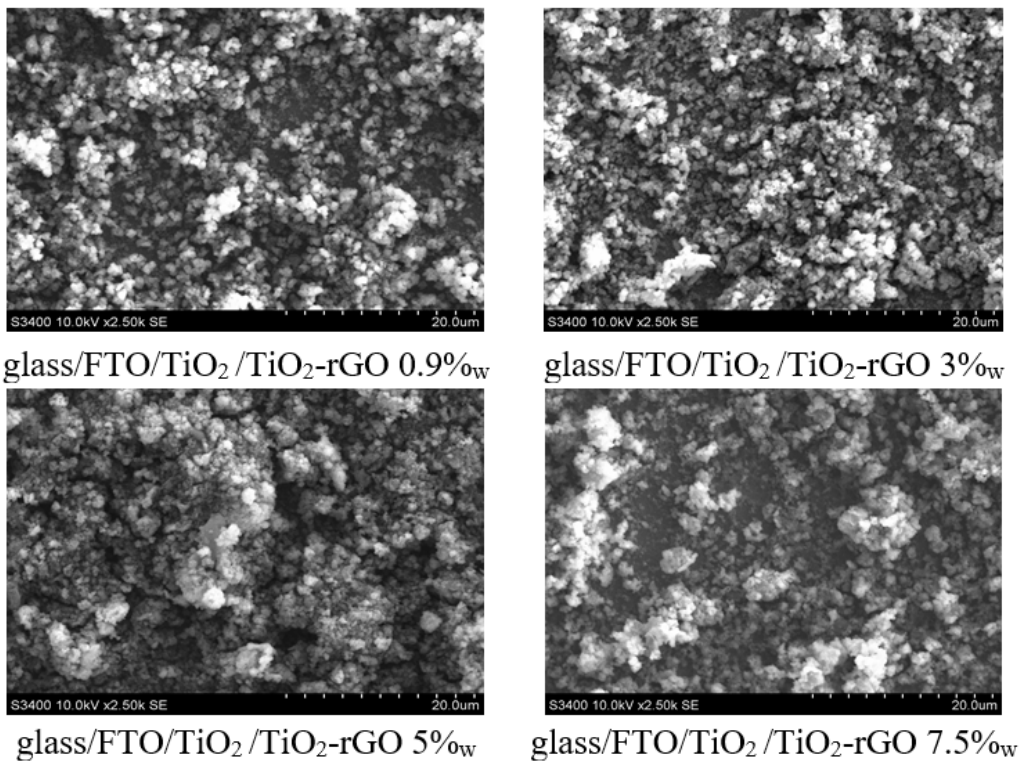


Fig. 4. SEM images of the double-layered composites with various rGO content.

Table 2. Surface elemental composition and roughness (RMS) values of the composites with 0.9%_w, 3%_w, 5%_w, 7.5%_w rGO content

Sample	Element[at%]				RMS[nm]
	C	Ti	O	SE*	
glass/FTO/TiO ₂ /TiO ₂ -rGO 0.9% _w	1.11	30.70	64.05	4.14	134.7
glass/FTO/TiO ₂ /TiO ₂ -rGO 3% _w	2.01	31.56	63.52	2.91	151.9
glass/FTO/TiO ₂ /TiO ₂ -rGO 5% _w	3.05	30.30	64.07	2.59	143.4
glass/FTO/TiO ₂ /TiO ₂ -rGO 7.5% _w	0.00	29.37	66.74	3.89	185.4

The surface elemental composition (Table 2) indicates a rather low overall carbon (C) content which constantly increases as the filler content increases, except for the 7.5%_w rGO sample, where the large and compact TiO₂ agglomerates may shield the carbon in the composite thin films, thus the results of the EDX tests. This additionally proves that, at this concentration, the rGO platelets are stacked and are not evenly distributed. A slightly higher titanium content than in the film only containing TiO₂ was recorded in all the composite thin films due to the aggregates deposited on the rGO platelets. Moreover, the content of the substrate elements (SE: Sn, F, Si) decreases as the rGO content increases up to 5%_w, suggesting that more uniform, denser and / or thicker thin films are obtained when a higher filler content is used in the thin composite layers. This does not apply to the 7.5%_w rGO composite thin film where the large agglomerates are

responsible for the cracks that leave the substrate surface more visible.

The RMS values inserted in Table 2 outline a relatively high roughness, particularly for the composite with 7.5%_w rGO in good agreement with the morphology images showing large aggregates at the sample surface. Following these results, this sample is expected to perform better in the photocatalysis processes, but the stability in the working conditions must be carefully considered.

These properties of the composite layers with TiO₂ matrix and rGO filler were correlated with the efficiencies recorded using these materials in the photocatalytic processes. The candidate that comes as the closest to the requirements for photocatalytic materials could be the one with 7.5%_w rGO due to the high RMS value that leads to a higher specific surface value that well supports the MB adsorption as first step in photocatalysis. However, the efficiency in the photocatalytic process and the stability in the aqueous environment has to be evaluated to support the selection of the optimum content of the rGO filler in the composite thin film.

Initial experiments investigated the sample with the lowest filler content (0.15%_w), thermally treated at 150° C to outline the Vis-activation even at a low filler percentage.

Table 3. Efficiencies of the photocatalytic and adsorption processes using composite thin films with 0.15%_w rGO content thermally treated at 150°C

Sample	Irradiation / Dark	Efficiency [%]			
		1 hour	2 hours	5 hours	9 hours
glass/FTO/TiO ₂ /TiO ₂ -rGO 0.15% _w 150TT	UV+VIS	7.40	9.48	18.30	27.74
	UV	7.93	8.39	14.21	20.53
	ADS	7.95	9.27	13.44	15.99

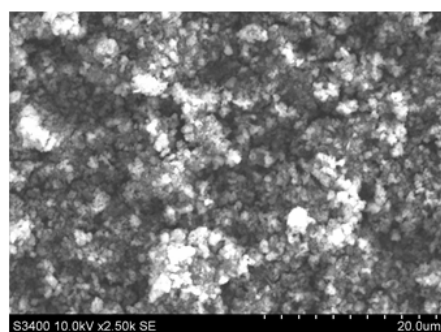
The results recorded in Table 3 outline the Vis-activation even at a low percentage of rGO. Subsequent experiments used samples with a rGO percentage in the composite up to 7.5%_w. The results after 1 hour in dark and 8 hours under UV+VIS or UV irradiation or in dark are inserted in Table 4.

Table 4. Efficiencies of the photocatalytic and adsorption processes using composite thin films with 0.15%_w rGO content thermally treated at 150°C

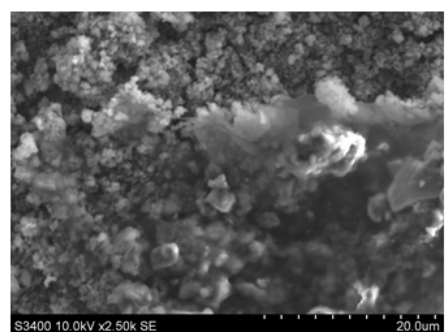
Sample	Photocatalytic efficiency [%]		Adsorption [%]
	UV+VIS	UV	
glass/FTO/TiO ₂ /TiO ₂ -rGO 0.9% _w	26.77	22.98	16.39
glass/FTO/TiO ₂ /TiO ₂ -rGO 3% _w	28.21	24.18	17.33
glass/FTO/TiO ₂ /TiO ₂ -rGO 5% _w	31.07	24.73	18.45
glass/FTO/TiO ₂ /TiO ₂ -rGO 7.5% _w	25.34	18.01	12.11

The higher efficiencies obtained using UV + VIS radiation compared to those recorded using UV confirm the Vis-activation of the thin films following the formation of the n-p heterojunction in the diode type composite structure. The results indicate a constant increase in the photo-degradation efficiency of MB when using the composite thin films up to a concentration of 5%_w rGO. At an rGO content higher than 5%_w, the MB photo-degradation efficiency was affected as adsorption is significantly decreased. The characterization results showed higher RMS values for the sample with the highest rGO concentration, but the film efficiency is lower thus the stability of the thin films has to be observed.

The stability of the thin films was evaluated based on the characterization results before and after UV+VIS photocatalysis starting with the sample with a low filler content (0.15%_w). The SEM images in Figure 5 correlated with the EDX results inserted in Table 5 allow concluding on the lower stability of these composites highlighted by the rGO platelets that were initially covered with TiO_2 surface aggregates. The results also indicate the increase in the carbon content after photocatalysis confirming the removal of the titania aggregates from the rGO platelets, thus this limited stability of the composite layer may be the result of the lower compatibility between the ionic matrix and the low polar rGO filler not uniformly distributed.



glass/FTO/ TiO_2 / TiO_2 -rGO 0.15%_w
150TT *before* photocatalysis



glass/FTO/ TiO_2 / TiO_2 -rGO 0.15%_w
150TT *after* UV+VIS photocatalysis

Fig. 5. SEM images of the double-layered composites with 0.15%_w rGO content thermally treated at 150°C, before and after UV+VIS photocatalysis.

Table 5. Elemental surface composition of the composites with 0.15%_w rGO thermally treated at 150°C, before and after UV+VIS photocatalysis

Sample	Element [at%]			
	C	Ti	O	F, Sn, Si, S (<i>after photocatalysis</i>)
glass/FTO/ TiO_2 / TiO_2 -rGO 0.15% _w 150TT before photocatalysis	1.01	34.01	64.54	0.44
glass/FTO/ TiO_2 / TiO_2 -rGO 0.15% _w 150TT after UV+VIS photocatalysis	10.47	27.20	58.27	4.06

The stability of the composite thin films with a higher rGO content (0.9%_w, 3%_w and 5%_w) was further evaluated. The SEM images in Figure 6 outline that the composite with a lower rGO content (0.9%_w) was mostly affected under the experimental conditions, as the rGO platelets appear on the composite surface while these were initially covered with TiO_2 aggregates. This is also confirmed by the decrease in the titanium content highlighted by the EDX results and the slight decrease in the RMS value (Table 6). These effects are less obvious in the samples with higher rGO content up to 5%_w, concluding that they may be better candidates as photocatalytic materials. The residual sulphur (S) content recorded on each film after the photocatalytic process outlines the need for periodical regeneration of the substrate after the process as potential by-

products from the MB oxidation may be adsorbed at the surface, regardless the rGO content.

Following the results recorded in Table 6, the sample with the highest stability was that containing 3%_w rGO followed by the thin film with 5%_w rGO concentration. Comparing the photocatalytic results, the highest process efficiency was recorded for the sample with 5%_w rGO in the composite layer (Table 4). The thin film selected to be recommended for up-scalable application(s) will have to consider all these results.

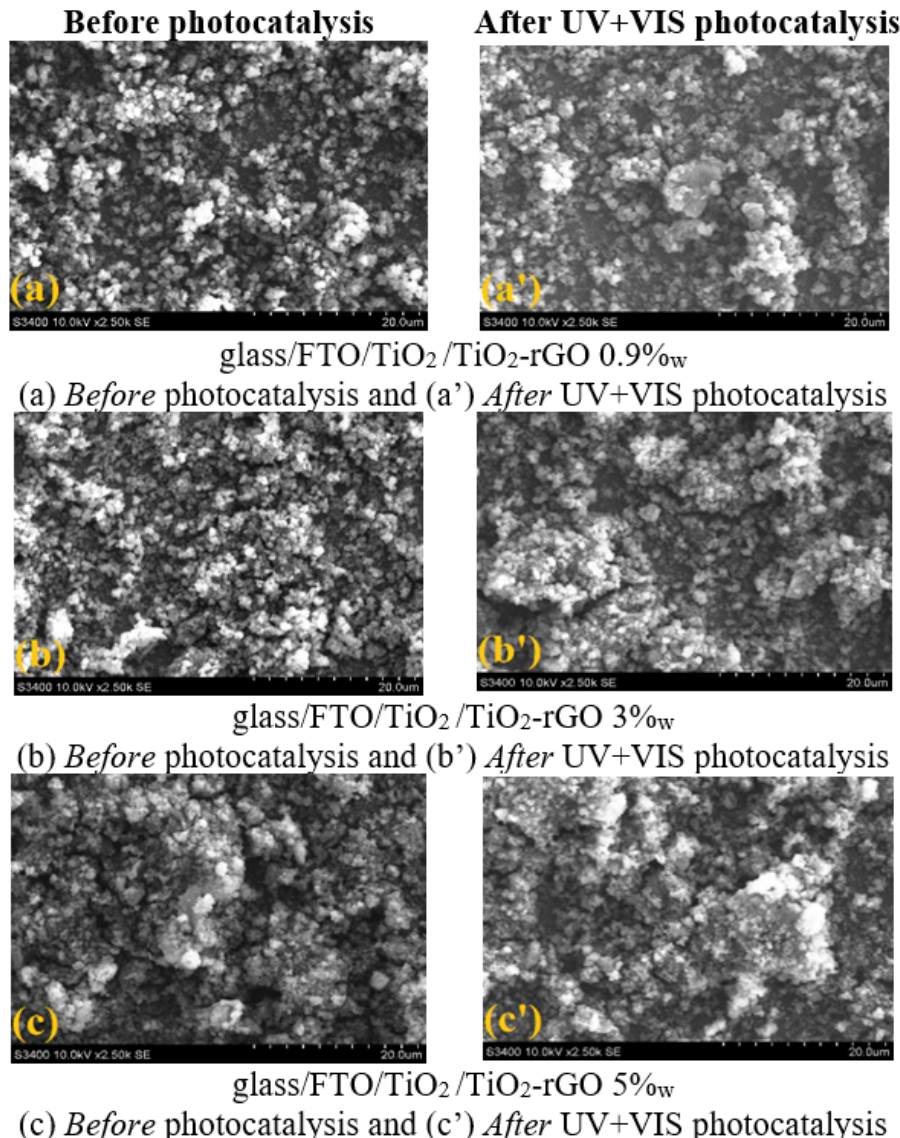


Fig. 6. SEM images of the double-layered composites thin films with 0.9%_w, 3%_w and 5%_w rGO content before and after UV+VIS photocatalysis, [9].

Table 6. Elemental surface composition and roughness (RMS) values of the composites with 0.9%_w, 3%_w, 5%_w rGO content before and after UV+VIS photocatalysis

Sample	Element[at%]					RMS[nm]
	C	Ti	O	SE*	S	
(a) glass/FTO/ TiO_2 / TiO_2 -rGO 0.9% _w before photocatalysis	1,11	30,70	64,05	4,14	-	134.7
(a') glass/FTO/ TiO_2 / TiO_2 -rGO 0.9% _w after UV+VIS photocatalysis	2,71	28,59	64,86	3,62	0,22	128.8
(b) glass/FTO/ TiO_2 / TiO_2 -rGO 3% _w before photocatalysis	2,01	31,56	63,52	2,91	-	151.9
(b') glass/FTO/ TiO_2 / TiO_2 -rGO 3% _w after UV+VIS photocatalysis	2,04	30,58	62,76	4,38	0,23	141.5
(c) glass/FTO/ TiO_2 / TiO_2 -rGO 5% _w before photocatalysis	3,05	30,30	64,07	2,59	-	143.4
(c') glass/FTO/ TiO_2 / TiO_2 -rGO 5% _w after UV+VIS photocatalysis	2,10	29,32	63,74	4,55	0,29	127.1

*SE: substrate elements (Sn, F, Si)

As the experiments using composites with a higher rGO content (7.5%_w) did not lead to higher MB removal efficiencies (according to the results in Table 4) and the thin films proved a relative low stability in the working conditions, it can be concluded that the optimal photocatalytic thin film with TiO_2 matrix and rGO filler has the structure: glass/FTO/ TiO_2 / TiO_2 -rGO 5%_w as this film outlined the highest efficiency in MB removal when irradiated with simulated solar radiation.

4. Conclusions

Double-layered composite thin films with TiO_2 matrix and rGO filler were deposited using spray pyrolysis deposition followed by sol spraying.

Initial experiments used composites with a low rGO filler content of 0.15%_w. Two temperatures (150°C and 200°C) were investigated for the final treatment, one below and one above the temperature considered to represent the thermal stability limit of rGO. The XRD patterns outline the characteristic peaks of the TiO_2 anatase polymorph and the peaks corresponding to the FTO substrate along with an additional peak corresponding to the filler; an acceptable crystallinity degree was recorded that well supports the charge carriers' mobility. The morphology shows large agglomerates of TiO_2 covering the rGO platelets and small cracks were observed on the thin films surface due to the reduced compatibility between the ionic metal oxide matrix and the almost non-polar rGO filler. The surface elemental composition demonstrates the lack of C content in the sample thermally treated at 200°C proving that the graphene derivative filler was decomposed at this temperature thus, the thermal treatment temperature was selected to be 150°C. The photocatalytic experiments in static regime using a 10 ppm solution of the MB pollutant under UV + VIS and UV radiation outlined the Vis-activation even at this low rGO content.

The rGO content was further increased in the composite layer to 0.9%_w, 3%_w, 5%_w and 7.5%_w rGO. The XRD patterns of all the thin films subject of investigation outline the TiO_2 peaks and the SnO_2 peaks from the glass/FTO substrate; moreover, the additional peak recorded

at 5.5° in the composite structures may be correlated with the rGO used as filler. The SEM images outline the deposition of the TiO₂ aggregates on top of the rGO platelets and continuous interfaces (especially for the films with 3%_w and 5%_w rGO) are formed while the EDX results outline a high Ti content at the surface following the stacked aggregates correlated with a low carbon content due to the well-covered rGO sheets. The roughness values confirm that these composites can well support the adsorption step in the photocatalytic process as rather high values were recorded for the composite thin films.

The photocatalytic efficiencies in MB photo-degradation confirm the Vis-activation as higher results were recorded when using UV+VIS radiation compared to UV. The experimental results outline the effect of the rGO content on the photocatalytic efficiencies: an increase in the efficiency was observed when increasing the rGO content up to 5%_w. At a higher filler content the results showed a decrease in the performance of the composite material, the adsorption step being mostly affected. The stability in the working environment was found to be the main cause for the lower efficiency recorded for the composite thin films with the highest rGO content (7.5%_w).

The stability of the photocatalytic thin films was evaluated based on the morphology, surface elemental composition and RMS variations and the results show that the samples with a low rGO content (0.15%_w and 0.9%_w) were mostly affected in the experimental conditions as a possible result of the less even distribution of the filler in the matrix. The thin films with higher rGO content (3%_w and 5%_w) proved to be significantly (more) stable; however, at higher concentrations (7.5%), the stability decreases correlated with the decrease in the composite efficiency in the photocatalytic process.

Following the photocatalytic efficiencies and the stability results, the thin film recommended to be further investigated at pilot scale is glass/FTO/TiO₂/TiO₂-rGO 5%_w (with 5%_w rGO content in the composite layer).

Acknowledgment. This work was supported by a grant of the Romanian Ministry of Research and Innovation, CCCDI – UEFISCDI, project number PN – III – P1 – 1.2 – PCCDI – 2017 – 0619, contract no. 42 PCCDI / 2018 within PNCDI.

References

- [1] K. E. DJEBBAR, A. ZERTAL, N. DEBBACHE and T. SEHILI, *Comparison of diuron degradation by direct UV photolysis and advanced oxidation processes*, Environmental Management **88**, pp. 1505–1512, 2008.
- [2] M. AQEEL, S. ANJUM, M. IMRAN, M. IKRAM, H. MAJEEED, M. NAZ, S. ALI and M. A. AHMAD, *TiO₂-rGO (reduced graphene oxide) doped nanoparticles demonstrated improved photocatalytic activity*, Materials Research Express **6**, 086215, 2019.
- [3] H. De LASA, B. SERRANO and M. SALAICES, *Photocatalytic reaction engineering*, Springer, New York, 2005.
- [4] M. HUMAYUN, F. RAZIQ, A. KHAN and W. LUO, *Modification strategies of TiO₂ for potential applications in photocatalysis: a critical review*, Green Chemistry Letters and Reviews **11**(2), pp. 86–102, 2018.
- [5] H. ZHANG, X. WANG, N. LI, J. XIA, Q. MENG, J. DING and J. LU, *Synthesis and characterization of TiO₂/graphene oxide nanocomposites for photoreduction of heavy metal ions in reverse osmosis concentrate*, RSC Advances **8**(60), pp. 34241–34251, 2018.

- [6] D. W. BOUKHVALOV and M. I. KATSNELSON, *Modeling of graphite oxide*, Journal of the American Chemical Society **130**, pp. 10697–10701, 2008.
- [7] A. TOLOSANA-MORANCHEL, M. FARALDOS, A. BAHAMONDE, L. PASCUAL, F. SIELAND, J. SCHNEIDER, R. DILLERT and D. W. BAHNEMANN, *TiO_2 -reduced graphene oxide nanocomposites: microsecond charge carrier kinetics*, Journal of Photochemistry and Photobiology A: Chemistry **386**, 112112, 2018.
- [8] INTERNATIONAL STANDARD ISO 10678:2010, Fine ceramics (advanced ceramics, advanced technical ceramics) Determination of photocatalytic activity of surfaces in an aqueous medium by degradation of methylene blue.
- [9] I. TISMANAR, A. C. OBRAJA, O. BUIU and A. DUTA, *TiO_2 - rGO composite thin films in Vis-active photocatalysis*, Proceedings of 2021 International Semiconductor Conference, Sinaia, Romania, pp. 31–34, 2021.
- [10] I. TISMANAR, A. C. OBRAJA, O. BUIU and A. DUTA, *VIS-active TiO_2 graphene oxide composite thin films for photocatalytic applications*, Applied Surface Science **538**, 147833, 2021.
- [11] L. YU, L. WANG, X. SUN and D. YE, *Enhanced photocatalytic activity of rGO/TiO₂ for the decomposition of formaldehyde under visible light irradiation*, Journal of Environmental Sciences **73**, pp. 138–146, 2018.